



**HAL**  
open science

## **Eggshell decalcification and skeletal mineralization during chicken embryonic development: defining candidate genes in the chorioallantoic membrane**

Maeva Halgrain, Nelly Bernardet, Marine Crepeau, Nathalie Mème, Agnès Narcy, Maxwell Hincke, Sophie Réhault-Godbert

### ► To cite this version:

Maeva Halgrain, Nelly Bernardet, Marine Crepeau, Nathalie Mème, Agnès Narcy, et al.. Eggshell decalcification and skeletal mineralization during chicken embryonic development: defining candidate genes in the chorioallantoic membrane. *Poultry Science*, 2022, 101 (2), pp.101622. 10.1016/j.psj.2021.101622 . hal-03457283

**HAL Id: hal-03457283**

**<https://hal.inrae.fr/hal-03457283>**

Submitted on 8 Jan 2024

**HAL** is a multi-disciplinary open access archive for the deposit and dissemination of scientific research documents, whether they are published or not. The documents may come from teaching and research institutions in France or abroad, or from public or private research centers.

L'archive ouverte pluridisciplinaire **HAL**, est destinée au dépôt et à la diffusion de documents scientifiques de niveau recherche, publiés ou non, émanant des établissements d'enseignement et de recherche français ou étrangers, des laboratoires publics ou privés.



Distributed under a Creative Commons Attribution - NonCommercial 4.0 International License

1 EGG SHELL DEMINERALIZATION DURING INCUBATION

2 **Eggshell decalcification and skeletal mineralization during chicken embryonic**  
3 **development: defining candidate genes in the chorioallantoic membrane**

4 Maeva Halgrain\*, Nelly Bernardet\*, Marine Crepeau\*, Nathalie Mème\*, Agnès Narcy\*,  
5 Maxwell Hincke<sup>#†</sup>, Sophie Réhault-Godbert\*

6

7 \*INRAE, Université de Tours, BOA, 37380, Nouzilly, France

8 #Department of Innovation in Medical Education, Department of Cellular and Molecular  
9 Medicine, Faculty of Medicine, University of Ottawa, Canada

10 †LE STUDIUM Research Consortium, Loire Valley Institute for Advanced Studies, Orléans-  
11 Tours, France,

12 Corresponding author:

13 Sophie Réhault-Godbert, INRAE, Université de Tours, BOA, 37380, Nouzilly, France, +33 2  
14 47 42 78 39, [sophie.rehault-godbert@inrae.fr](mailto:sophie.rehault-godbert@inrae.fr)

15 Scientific section: Physiology and Reproduction

16

17 **ABSTRACT**

18 During chicken embryonic development, skeleton calcification mainly relies on the eggshell,  
19 whose minerals are progressively solubilized and transported to the embryo *via* the  
20 chorioallantoic membrane (**CAM**). However, the molecular components involved in this  
21 process remain undefined. We assessed eggshell demineralization and calcification of the  
22 embryo skeleton after 12 and 16 days of incubation, and analyzed the expression of several  
23 candidate genes in the CAM: carbonic anhydrases that are likely involved in secretion of  
24 protons for eggshell dissolution (CA2, CA4, CA9), ions transporters and regulators (CALB1,  
25 SLC4A1, ATP6V1B2, SGK1, SCGN, PKD2) and vitamin-D binding protein (GC).

26 Our results confirmed that eggshell weight, thickness and strength decreased during incubation,  
27 with a concomitant increase in calcification of embryonic skeletal system. In the CAM, the  
28 expression of CA2 increased during incubation while CA4 and CA9 were expressed at similar  
29 levels at both stages. SCL4A1 and SCGN were expressed, but not differentially, between the  
30 two stages, while the expression of ATP6V1B2 and PKD2 genes decreased. The expression of  
31 SGK1 and TRPV6 increased over time, although the expression of the latter gene was barely  
32 detectable. In parallel, we analyzed the expression of these candidate genes in the yolk sac (**YS**),  
33 which mediates the transfer of yolk minerals to the embryo during the first half of incubation.  
34 In YS, CA2 expression increases during incubation, similar to the CAM, while the expression  
35 of the other candidate genes decreases. Moreover, CALB1 and GC genes were found to be  
36 expressed during incubation in the YS, in contrast to the CAM where no expression of either  
37 was detected.

38 This study demonstrates that the regulation of genes involved in the mobilization of egg  
39 minerals during embryonic development is different between the YS and CAM extraembryonic  
40 structures. Identification of the full suite of molecular components involved in the transfer of

41 eggshell calcium to the embryo via the CAM should help to better understand the role of this  
42 structure in bone mineralization.

43 **Key words:** chicken, eggshell, embryo, mineral, chorioallantoic membrane

44

45

## INTRODUCTION

46 The nutrient reserve of the fertile egg consists of three distinct compartments that are  
47 progressively mobilized to support embryonic development: the yolk, the albumen and the shell  
48 (Romanoff, 1960; Romanoff and Romanoff, 1967; Bellairs and Osmond, 2014). During  
49 incubation, these nutrient reservoirs operate dynamically and serve at different stages of growth  
50 to meet embryo requirements for lipids, amino acids, carbohydrates, and minerals. When  
51 focusing on mineral ions, the shell is the main source of Ca, Mg, and Sr; the albumen is the  
52 major source of K and Na; and the yolk provides Cu, Fe, Mn, P, and Zn (Richards, 1997;  
53 Schaafsma et al., 2000; Yair and Uni, 2011; Hopcroft et al., 2019). Many studies indicate the  
54 importance of egg mineral ions for the development of the embryo but also for the skeletal  
55 health of chick and adult birds. In fact, a mineral deficiency has adverse repercussions on  
56 skeletal, immune and cardiovascular systems, reduces hatchability and increases mortality  
57 (Richards, 1997; Kidd, 2003; Angel, 2007; Dibner et al., 2007). The transfer of minerals from  
58 the yolk during the first half of incubation, and from the eggshell during the second half of  
59 incubation to the embryos (Romanoff, 1960), intrinsically depends on the functionality of extra-  
60 embryonic structures, namely the yolk sac (**YS**) for the yolk and the chorioallantoic membrane  
61 (**CAM**) for the eggshell.

62 During embryonic development, nutrients are transferred from the yolk contents to the embryo  
63 through the yolk sac membrane (**YSM**) and its surrounding vascular system (Uni et al., 2012).

64 From embryonic day (**ED**) 19, the YS begins to be internalized into the abdominal cavity of the

65 embryo and residual yolk provides critical nutrients until hatched chicks have access to food  
66 (Romanoff, 1960). It has been shown that the YSM expresses digestive enzymes and nutrient  
67 transporters similarly to the intestine (Speake et al., 1998; Yadgary et al., 2011; Yair and Uni,  
68 2011; Speier et al., 2012; Bauer et al., 2013; Yadgary et al., 2014). Yair and Uni (2011)  
69 observed that the total calcium content of the yolk (30 mg at D0) decreases during the first half  
70 of incubation to reach a plateau from ED11 (20 mg) until hatch. During the second half of  
71 incubation, the eggshell becomes a major contributor of calcium for supporting skeletal  
72 mineralization of the embryo (Yair and Uni, 2011). The solubilization of eggshell minerals and  
73 the transfer of eggshell calcium to the embryo is ensured by the CAM, which is a highly  
74 vascularized structure that lines the inner eggshell and develops from ED5 onwards (Romanoff,  
75 1960). The CAM is complete by ED10-11, grows rapidly from ED11 to ED15-16, and starts to  
76 degrade from day 19 onwards (Romanoff, 1960; Leeson and Leeson, 1963; Narbaitz and  
77 Tellier, 1974; Makanya et al., 2016). The CAM is fully differentiated at ED15-16 and is  
78 composed of three distinct cellular structures, namely the chorionic epithelium, the mesoderm  
79 and the allantoic epithelium (Makanya et al., 2016), all of which are assumed to play different  
80 but complementary roles. The chorionic epithelium participates in acid-base balance of the  
81 embryo and mineral solubilization and transport from the eggshell (Gabrielli and Accili, 2010).  
82 The mesoderm is the site of early development of the extraembryonic vascular system, which  
83 serves the CAM epithelia and forms the chorionic capillary plexus to facilitate gaseous  
84 exchange (Melkonian et al., 2002). The allantoic epithelium is involved in ion and H<sub>2</sub>O  
85 reabsorption from the allantoic fluid and maintains the acid-base balance of this fluid (proton  
86 secretion and bicarbonate reabsorption) (Stewart and Terepka, 1969; Narbaitz, 1995). Hence,  
87 the CAM is involved in the dissolution and transport of calcium from the eggshell to the  
88 embryo, gaseous exchange, maintenance of acid-base balance, water and electrolyte  
89 reabsorption from the allantoic cavity and innate immunity (Romanoff, 1960; Coleman and

90 Terepka, 1972a, b; Gabrielli and Accili, 2010; Hincke et al., 2019). Only a few candidate  
91 proteins in the CAM have been proposed to participate in eggshell solubilization and mineral  
92 ion transport to date: a calbindin-like protein, an anion exchanger (AE1), a H<sup>+</sup>-ATPase, and  
93 soluble and membrane-bound isoforms of carbonic anhydrase (Tuan and Zrike, 1978; Rieder et  
94 al., 1980; Anderson et al., 1981; Narbaitz et al., 1981; Tuan, 1984; Tuan et al., 1986; Narbaitz  
95 et al., 1995; Gabrielli et al., 2001; Gabrielli, 2004; Gabrielli and Accili, 2010). Moreover, the  
96 identity of the associated genes remains ambiguous and depends on the annotated chicken  
97 genome assemblies used as a reference [Galgal4 (GCA\_000002315.2) in 2013, Gallus\_gallus-  
98 5.0 (GCA\_000002315.3) in 2016, GRCg6a (GCA\_000002315.5) in 2018] (Peona et al., 2018)].  
99 In this work, we studied the expression of 10 candidate genes in the CAM and YS at ED12  
100 (CAM is developed but not fully mature), and at ED16 (corresponding to a fully differentiated  
101 stage). The demineralization of the eggshell as well as the calcification of the embryo skeleton  
102 have been assessed in parallel to further appreciate the interrelationship between these two  
103 physiological processes. The data obtained in this article revisit some of the statements from  
104 the literature and show for the first time that the molecular components involved in mineral  
105 mobilization from the yolk and the eggshell are different.

106

107

## MATERIALS AND METHODS

### *Incubation Procedures and Sample Collection*

109 Sixty fertilized eggs were obtained from 29-wk old laying hens (Rhode Island Red, Novogen,  
110 France) and handled in the Poultry Experimental Facility (PEAT) UE1295 (INRAE, F-37380  
111 Nouzilly, France, DOI: 10.15454/1.5572326250887292E12). Eggs were incubated under  
112 standard conditions (45% RH, 37.8°C, automatic turning every hour; Bekoto B64-S, Pont-  
113 Saint-Martin, France), after a 3-day storage at 16°C, 85% RH to favor synchronization of

114 developmental stages. For each embryonic day studied (ED12 and ED16), 30 eggs (64.1±1.8g)  
115 containing viable embryos were selected. At each stage, egg weight and eggshell strength were  
116 measured prior to tissue sampling (Digital Egg Tester 6000, Nabel, Kyoto, Japan). Eggs were  
117 opened at the air chamber end and the egg contents were poured into a Petri dish. Embryos were  
118 sacrificed by decapitation, and placed in a sterile flask containing 75 ml of 90% ethanol prior  
119 to staining (see below). The yolk sac and the chorioallantoic membrane were removed, washed  
120 several times with sterile saline solution (NaCl 0.9%), immersed in liquid nitrogen and stored  
121 at -80°C. Eggshell thickness was measured using a small piece of eggshell (Digital Egg Tester  
122 6000, Nabel, Kyoto, Japan) and eggshell weight was obtained after drying for 2 hours at 110°C.  
123 Resulting eggshells were further stored at 4°C prior to analysis of mineral content. These  
124 experiments performed on embryos at day 12 and day 16 of development were conducted in  
125 compliance with the European legislation on the “Protection of Animals Used for Experimental  
126 and Other Scientific Purposes” (2010/63/UE) and under the supervision of an authorized  
127 scientist (S. Réhault-Godbert, Authorization no. 37-144). These experiments meet the  
128 guidelines approved by the institutional animal care and use committee (IACUC).

129

### 130 ***Alizarin Red S (Bone) and Alcian Blue (Cartilage) Staining of Chicken Embryos***

131 Chicken embryo bone and cartilage staining was performed as described for mouse embryos  
132 (Scientific Protocols, 2014) with some small adjustments. After sampling, embryo bodies were  
133 fixed in 90% ethanol for 11 days at 4°C with renewal of the solution every 4 days. Skin, viscera,  
134 liver, kidney and gut were removed. Embryos were placed in an Alcian blue solution (0.1g/L)  
135 (Sigma, Saint-Louis, USA, ref. A5268) for 3 days, followed by rehydration with several baths  
136 of decreasing percentages of ethanol (from 70% to 0% in demineralized water; 70% during 2  
137 hours/ 40% during one night/ 15% during 2 hours and finally, demineralized water for 4 hours).  
138 The clearing of embryos was achieved with 1% KOH solution for 2 days and the staining of

139 mineralized structures was performed during 3 days in Alizarin red / KOH solution at 0.01 g/L  
140 (Sigma, Saint-Louis, USA, ref. A5533). Stained embryos were rinsed in 1% KOH, followed by  
141 increasing solutions of glycerol (20 to 80%, over 5 days) / 1% KOH, before storage at 4°C in  
142 100% glycerol. Stained ED12 and ED16 embryos were analyzed visually and photographed  
143 (Nikon apparatus D5100, Itteville, France). Identification of bones was based on the Atlas of  
144 Chick Development (plates 230 and 231, Bellairs and Osmond, 2014).

145

#### 146 ***Eggshell Mineral Content***

147 Eggshell mineral quantification was performed according to Park and Sohn (2018), with small  
148 adjustments. Eggshell fragments were washed, dried, weighed and then grinded using a  
149 Cryomill ball mill (Retsch, Haan, Germany). Eggshell powder (300 mg) was dissolved in 10  
150 mL of 65% nitric acid, and then heated / digested in a microwave for 15 min at 200°C, 1800 W  
151 (Ethos Up, Milestone, Sorisole, Italy). Total P, Mg, K, Na and Ca were determined using an  
152 inductive coupled plasma atomic emission spectrometer (ICP OES Thermoscientific™  
153 iCAP™ 7200; method 990.08; AOAC International, 2006). Standard solutions (P, Mg, K, Na  
154 and Ca) were prepared from a 1,000 mg/mL stock solution (Certipur® Merck, Darmstadt,  
155 Allemagne). All assays were performed in duplicates.

156

#### 157 ***mRNA extraction and real-time quantitative PCR***

158 All tissue samples (n=18 per stage, ED12 and Ed16) were homogenized in liquid nitrogen with  
159 a mechanical crusher A11 Basic (IKA, Staufen im Breisgau, Germany). For CAM samples,  
160 total RNA was extracted using the Nucleospin RNA kit according to the manufacturer's  
161 recommendations (Macherey-Nagel, Düren, Germany). For yolk sac samples, total RNA was



162 extracted using RNeasy® Lipid Tissue Mini Kit, according to the manufacturer's  
163 recommendations (Qiagen, Hilden, Germany).

164 To remove traces of genomic DNA, a second treatment with DNase was performed on all  
165 samples (kit Turbo DNA-free™, Life Technologies, Carlsbad, USA). Concentration and  
166 quality of the extracted RNA were assessed by spectrophotometry (Nanodrop 1000  
167 spectrophotometer Nanodrop Technology, Wilmington, USA) and by migration of total RNA  
168 on a 1% agarose gel. Total RNA samples (1 µg) were reverse transcribed using RNase H-  
169 MMLV reverse transcriptase (Superscript™ II RT, Invitrogen, Cergy Pontoise, France). Gene  
170 quantification was achieved by SYBR Green incorporation, using LightCycler 480 (Roche,  
171 Mannheim, Germany).

172 Candidate genes to be analyzed were selected according to the literature (Gabrielli, 2004;  
173 Gabrielli and Accili, 2010). Other studies related to eggshell calcification or intestinal calcium  
174 transporters in chickens provided additional candidates (Jonchère et al., 2012; Gloux et al.,  
175 2019; Gautron et al., 2021). The list of candidate genes is presented in Table 1.

176

### 177 ***Calculation of Relative Gene Expression***

178 The relative normalized expression ( $R$ ) of a candidate gene was calculated, based on the  
179 Efficiency ( $E$ ) and the cycle threshold ( $C_t$ ) deviation of cDNA samples (CAM or YS at ED12  
180 and ED16 from individual embryos) vs. a calibrator. The calibrator corresponds to the pool of  
181 cDNA from all CAM samples (CAM analysis) or a pool of cDNA from all YS samples (YS  
182 analysis). Data were expressed relative to the normalization factor of housekeeping genes  
183 calculated by GeNorm (version 3.5) (Vandesompele et al., 2002). Briefly, normalized  
184 quantities were calculated using the following formula:  $\text{gene efficiency}^{(C_{t\text{calibrator}} -$

185 Ctsample) / normalization factor of each sample (calculated based on geometric mean of  
186 housekeeping genes).

187 Five stable housekeeping genes could be utilized for CAM samples, while for the yolk sac, only  
188 one gene (ACTB) was shown to be invariant between stages and thus was selected for  
189 calculation of relative expression. The selected housekeeping genes were:

190 ACTB (Gene ID : 396526, Actin, Beta; Forward CTGGCACCTAGCACAATGA; Reverse  
191 CTGCTTGCTGATCCACATCT); PPIA (Gene ID : 776282, Peptidylpropyl isomerase A;  
192 Forward : CGCTGACAAGGTGCCCATAA; Reverse : GTCACCACCCTGACACATGA);  
193 STAG2 (Gene ID : 422360, Stromal antigen 2; Forward: GCACACACCAGTCATGATGC;  
194 Reverse: TGGTGTTCAGGCTGCATAGG) ; TBP (Gene ID : 395995, TATA-box binding  
195 protein; Forward: GCGTTTTGCTGCTGTTATTATGAG; Reverse:  
196 TCCTTGCTGCCAGTCTGGAC); YWHAZ (Gene ID : 425619, Tyrosine 3-  
197 monooxygenase/tryptophan 5-monooxygenase activation protein zeta; Forward:  
198 TGCTGCTGGAGATGACAAGA, Reverse: AGGCCTTCTCTGGGGAATTG).

199

## 200 *Statistical Analyses*

201 All statistical analyses were performed using R Software, version 4.0.2 (R Core Team, 2017,  
202 Vienna, Austria). Because the samples were not normally distributed (Shapiro test), statistical  
203 analyses were performed using a Wilcoxon test (P<5%).

204

## 205 **RESULTS**

### 206 *Eggshell Physical Characteristics and Mineral Content*

207 The effect of incubation on the eggshell quality parameters and mineral ion content (phosphorus  
208 (P), magnesium (Mg), potassium (K), sodium (Na) and calcium (Ca)) are shown in Table 2.  
209 The following parameters decreased the egg and eggshell weights, breaking strength and  
210 thickness all decrease significantly from ED12 to ED16 ( $P=0.034$ ,  $P=0.0133$ ,  $P<0.0001$ ,  
211  $P<0.0001$ , respectively). Concomitant to the decrease in eggshell weight, we observed a  
212 significant decrease in the total content of Mg, Na and Ca between ED12 and ED16 ( $P=0.0112$ ,  
213  $P=0.0307$  and  $P<0.01$ , respectively).

214

### 215 *Kinetic of skeleton Mineralization*

216 The typical staining pattern of embryo skeletons with Alcian blue (a cationic dye that binds  
217 glycosaminoglycans and sulfated glycoproteins in cartilage) and Alizarin red (an anionic dye  
218 that binds cationic calcium and calcium deposits) at ED12 (A) and ED16 (B) is presented in  
219 Figure 1. The wing and leg bones are already partially mineralized at ED12 (humerus, radius,  
220 ulna, and femur, tibiotarsus, respectively), while calcification of the ribs is initiated at ED12  
221 and complete around ED16. Some skeletal regions corresponding to the cervical vertebra, the  
222 ribs, the pelvic bones (ilium, ischium, pubis, caudal vertebra) and the digits of the legs exhibit  
223 a visually apparent increase in mineralization between these stages (Figure 1).

224

### 225 *Relative Expression of Candidate Genes in the Yolk Sac and the CAM*

226 The mRNA expression of eight candidate genes in both the CAM and the yolk sac is presented  
227 in Figures 2A and 3A. Three genes that are specifically expressed in the CAM but not the YS  
228 (TRPV6), and in the yolk sac but not in the CAM (CALB1 and GC), are presented in Figure  
229 2B and 3B, respectively.

230 In the CAM, the expression of **CA2**, **SGK1** and **TRPV6** are higher at ED16 (about 2 fold,  
231  $P < 0.001$ ) while the expression of **PKD2** and **ATP6V1B2** decreases (about 1.4 fold) between  
232 ED12 and ED16 ( $P < 0.01$  and  $P < 0.05$ , respectively). The incubation stage has no effect on the  
233 mRNA expression of carbonic anhydrase 9 and 4 (**CA9** and **CA4**), **SLC4A1** or **SCGN**.

234 In the yolk sac, stage of development does not affect **PKD2** expression (Figure 3A) while the  
235 expression of **CA2** and **CALB1** increases when comparing ED16 to ED12 (15-20 fold,  
236  $P < 0.001$ ) (Figure 3A and 3B, respectively). The relative expression of other candidate genes  
237 (**CA9**, **CA4**, **SLC4A1**, **ATP6V1B2**, **SGK1**, **SCGN**, and **GC**) decreases during incubation (up  
238 to a 20-fold decrease depending on the gene,  $P < 0.001$ ).

239

240

## DISCUSSION

### 241 *The Alteration in Eggshell Integrity Reflects Mineral Release*

242 In birds, the egg contains all the protective and nutritive elements to ensure the development of  
243 the embryo until hatching. The eggshell is a physical barrier that protects the embryo from  
244 environmental changes and microbes. It also regulates gaseous exchange through its pores  
245 while limiting water loss, and provides most of the calcium that is necessary for mineralization  
246 of the embryonic skeleton (Nys et al., 2010). The yolk contains about 30 mg of calcium while  
247 up to 800 mg of eggshell calcium are resorbed from the day of lay to the day of hatch (Yair and  
248 Uni, 2011). Such amounts may slightly differ depending on initial egg weight. The decrease in  
249 eggshell weight is essentially observed during the second half of incubation when the embryo  
250 skeleton needs to be reinforced to support a 5-fold increase of the embryo body weight (from 5  
251 g at ED11 to 25 g at ED18) (Makanya et al., 2016). In our experiment, between ED12 and  
252 ED16, eggshell loss is about 300 mg, corresponding to 120 mg of calcium (Table 2). The  
253 eggshell ultrastructure is complex, and is characterized (from inside to outside) by the

254 mammillary layer (where biomineralization is initiated), the palisade layer (responsible for most  
255 of the eggshell thickness and resistance to fracture), the vertical crystal layer and the cuticle. It  
256 has been reported that eggshell resorption mainly occurs from the calcium reserve body in the  
257 shell mammillary region (Tyler and Simkiss, 1959; Simons, 1971; Bond et al., 1988), and  
258 progressively induces the detachment of eggshell membranes together with erosion of the  
259 mammillary knobs (Simons, 1971; Bond et al., 1988; Chien et al., 2009). The loss of eggshell  
260 mineral and the weakening of the underlying support for the thick palisade layer likely explains  
261 the decrease in eggshell thickness and associated strength, as observed in Table 2. Such eggshell  
262 thinning may result in an increased susceptibility to penetration by environmental microbes,  
263 but concomitantly facilitates chick emergence (Hincke et al., 2019). Previous publications have  
264 reported that although the eggshell is 96% calcium carbonate, the distribution of minor mineral  
265 ions is heterogeneous: the Mg concentration is higher in the mammillary layer and at the outer  
266 palisade layer, while phosphorus (as inorganic phosphate or associated with phosphoproteins)  
267 is mainly incorporated during the eggshell termination process and is found in the outer palisade  
268 layer and cuticle (Cusack et al., 2003; Shen and Chen, 2003; Hincke et al., 2012). Calcium  
269 carbonate is deposited constantly throughout the process of eggshell formation (Waddel et al.,  
270 1989; Waddel et al., 1991; Shen and Chen, 2003; Gautron et al., 2021). Regulation of this  
271 process by the organic matrix results in the distinctive ultrastructure and microstructure of the  
272 eggshell (Dennis et al., 1996; Hincke et al., 2012; Rodriguez-Navarro et al., 2015; Gautron et  
273 al., 2021). The innermost layer that is in contact with the eggshell membranes is named the  
274 mammillary layer; each mammillary cone consists of a base plate that is the calcified foundation  
275 of the eggshell, a calcium reserve body, a cover and a crown. The calcium reserve body is  
276 described as the main source of calcium which is mobilized for skeletal mineralization during  
277 embryonic development (Dennis et al., 1996; Chien et al., 2008). A positive correlation is  
278 observed between the number of mammillary tips and calcium removal from the eggshell

279 (Karlsson and Lilja, 2008). In line with previously published data (Schaafsma et al., 2000), our  
280 results show that eggshell mineral (approximately 96% calcium carbonate) is composed of  
281 calcium (364 mg/g of eggshell) and magnesium (3.11 mg/g of eggshell) as its main cations, but  
282 also phosphate (1.08 mg/g of eggshell) (Table 2). In our experiment, the decrease in eggshell  
283 weight is associated with the decrease in calcium, magnesium and sodium but not in potassium  
284 and phosphorus (Table 2). These data suggest that potassium and phosphorus are concentrated  
285 in the outermost and intermediate layers of the eggshell that are not resorbed during incubation.  
286 Indeed, phosphate was described previously to regulate the termination of eggshell formation,  
287 which is consistent with its outer localization (Gautron et al., 1997; Cusack et al., 2003). These  
288 findings underline that eggshell phosphate is not required for bone mineralization, which  
289 supports the general statement that the phosphate reservoir for the embryo is the yolk, with  
290 about 180 mg at ED0 (Romanoff and Romanoff, 1967), and not the eggshell (Tuan and Ono,  
291 1986; Chien et al., 2009).

292 The staining of the embryos collected at ED12 and ED16 with Alcian blue and Alizarin red  
293 (Figure 1) showed that long bones are already partially mineralized at ED12, which  
294 corroborates previous studies: the tibial calcium content begins to increase from 12 days of  
295 incubation to reach maximum values around ED19 (Kubota et al., 1981; Torres and Korver,  
296 2018). This increase in bone calcification occurs in parallel with bone citrate decarboxylation  
297 and alkaline phosphatase activities, both reflecting osteoblast activity. These activities start to  
298 increase around ED10-12, reach a peak at ED19, and then decrease, and are strongly correlated  
299 with calcium-binding activity in the chorioallantoic membrane (Kubota et al., 1981). From  
300 embryonic stages ED14 to ED19, chicken long bones roughly double their length, thickness  
301 and total amount of bone mineral (Yair et al., 2012; Bellairs and Osmond, 2014), in order to  
302 support the rapid growth of the embryo. These structural modifications require massive  
303 transport of calcium from the eggshell and phosphorous from the yolk (Yair and Uni, 2011),

304 through the substantial vasculature of the CAM and of the YS. Kerschnitzki et al. (2016)  
305 reported the presence of membrane-bound mineral particles (calcium and phosphorus) in blood  
306 vessels during long bone development of chicken embryos, and it is generally observed that  
307 osteogenesis is coupled with angiogenesis during this process (Kusumbe et al., 2014). Between  
308 ED12 and ED16, a constant decrease in blood  $\text{Ca}^{2+}$  (measured via the allantoic vein) is  
309 accompanied by an increase in tibial mineral calcium, which collectively corroborates the rapid  
310 assimilation of circulating  $\text{Ca}^{2+}$  for bone mineralization (Everaert et al., 2008).

311 The transfer of calcium from the eggshell to the embryo is mediated by a three-layer structure,  
312 namely the chorioallantoic membrane. The chorionic epithelium of the CAM lines the eggshell  
313 membranes and is involved both in the solubilization of calcium from the inner eggshell, and  
314 in the transfer of solubilized ions to the embryo via its capillary network.

315

316 *The CAM expresses carbonic anhydrases and ion-binding proteins but not calbindin*  
317 *(CALBI) nor vitamin-D binding protein (GC)*

318 Distinct and specialized cell types characterize the mature chorionic epithelium: the villus  
319 cavity (VC) cells and the capillary covering (CC) cells (Figure 4A). Previous publications have  
320 shown that the major molecular components for extracellular acidification adjacent to the  
321 eggshell are localized within the VC cells (Figure 4A). These are the AE1 anion exchanger  
322 (AE1, possibly corresponding to SLC4A1), a cytoplasmic carbonic anhydrase 2 (CA2), a  
323 membrane-bound carbonic anhydrase, and a  $\text{H}^+$  ATPase (Gabrielli and Accili, 2010); however,  
324 except for CA2, the identity (i.e. gene ID) of most these major proteins remains undetermined.  
325 In this context and based on information available in the literature, we investigated the  
326 expression of 10 candidate genes in the CAM. Our results showed that the expression of CA2  
327 increases over time as previously published (Tuan and Zrike, 1978), but we also showed for the

328 first time that CA4 and CA9 are constantly expressed between ED12 and ED16 (Figure 2).  
329 Indeed, carbonic anhydrases have been reported to play a major role in proton secretion for  
330 solubilization of the eggshell mineral calcite via VC cells (Tuan and Zrike, 1978; Rieder et al.,  
331 1980; Anderson et al., 1981; Narbaitz et al., 1981; Tuan, 1984; Tuan et al., 1986; Narbaitz et  
332 al., 1995; Gabrielli et al., 2001; Gabrielli and Accili, 2010). Noticeably, CA2 was also  
333 previously identified in mitochondria-rich cells (MRC) that are highly concentrated in the  
334 allantoic epithelium (Narbaitz et al., 1995; Gabrielli et al., 2001). This protein is assumed to  
335 participate in maintaining acid-base homeostasis in the allantoic fluid during embryonic  
336 development. Carbonic anhydrases catalyze the reversible hydration of carbon dioxide to  
337 produce protons and bicarbonate ions and, in parallel, are thought to regulate several  
338 bicarbonate transporter activities. SLC4A1 (AE1) is continuously expressed between the two  
339 stages and may transport bicarbonate ions into cells, to maintain an extracellular acidic  
340 environment, but also into erythrocytes, where bicarbonate ions accumulate between ED10 and  
341 ED16 of incubation (Everaert et al., 2008). Besides VC cells, both CA2 and SLC4A1 were  
342 reported to be expressed in erythrocytes to contribute to blood homeostasis. A vacuolar H<sup>+</sup>  
343 ATPase was also previously described as participating in the extracellular proton flux. In our  
344 experiment, the subunit ATP6V1B2 was shown to be expressed in the CAM but its expression  
345 decreased modestly over time, which is not in accordance with the increased concentration of  
346 intracellular protons. However, the profile of expression of ATP6V1B2 between ED12 and  
347 ED16 resembles the activity profile of a proton pump that was described to be calcium-  
348 dependent (Tuan and Knowles, 1984). The activity of this protein followed a bimodal pattern  
349 with a decrease from day ED12 to ED16 followed by an increase essentially after ED16 of  
350 incubation to reach a maximum value around hatch (Tuan and Knowles, 1978).

351 We have shown above that ED16 is characterized by the loss of calcium, sodium and  
352 magnesium from the eggshell (Table 1). Ion transfers and exchanges are believed to be



353 mediated by the so-called capillary covering cells (CC cells, Figure 4A). Although we did not  
354 explore magnesium-binding proteins and transporters, we identified SCGN whose expression  
355 remains stable over time, and TRPV6 that is slightly overexpressed at ED16, as potential  
356 calcium-binding proteins. Surprisingly, when looking at calcium-binding proteins, we found  
357 that SCGN expression level remains stable between ED12 and ED16, while TRPV6 expression  
358 is low and no expression of CALB1 could be detected. Altogether, these data suggest that other  
359 not yet identified calcium-binding proteins are responsible for ion movements in the CAM. An  
360 alternative hypothesis is that the calcium flux in the cells and subsequently in the blood, does  
361 not involve calcium-binding proteins at this stage but maybe later during the time course of  
362 development. Indeed, calcium-binding activity has been shown to be maximal at day 18 (6-fold  
363 increase between ED15 and ED18) (Torres and Korver, 2018). The resulting high intracellular  
364 calcium concentration is likely to downregulate PKD2 expression. Our hypothesis is that the  
365 lower expression of PKD2 (a regulator of intracellular calcium signaling) may reflect the  
366 necessity of CC cells to concentrate high intracellular calcium without triggering cellular  
367 pathological signaling through an undesired PKD2 activation. The regulation of sodium flux  
368 may involve SGK1, which is localized in the nucleus, but also in mitochondria and the plasma  
369 membrane, and that is an important regulator of ion channels, including sodium channels (Lang  
370 and Shumilina, 2013). This gene was shown to be overexpressed in the CAM during incubation  
371 and may potentially be localized in CC cells but also in erythrocytes, as previously reported  
372 (Maizels, 1954; Clarkson and Maizels, 1955). A schematic representation of the expression  
373 pattern of candidate genes in the chorionic epithelium of the CAM is illustrated in Figure 4A.  
374 Noticeably, the allantoic epithelium is also likely to be involved in the assimilation of calcium  
375 and phosphate that accumulate in the allantoic fluid owing to the large increase in embryo  
376 metabolism during the second half of incubation (Everaert et al., 2008). The absence of GC  
377 (vitamin D transport protein) expression in the CAM at these two stages is consistent with the

378 fact that calcium transport and uptake by the CAM were not regulated by vitamin D (Packard  
379 et al., 1998).

380

381 *The YS expresses CA2, calbindin (CALB1) and vitamin-D binding protein (GC)*

382 In the YS, a variety of expression patterns were observed for the genes under study. Most of  
383 the candidate genes demonstrated a decrease in expression between ED12 and ED16; however,  
384 CA2 expression increased similarly to the CAM during incubation, PKD2 did not exhibit any  
385 difference in expression between the two stages, and TRPV6 was not expressed at either stage  
386 (Figure 4B). Carbonic anhydrases were demonstrated to be important in the formation of  
387 subembryonic fluid in early Japanese quail and turkey embryos and are localized in the  
388 endoderm of yolk sac during the early stages of incubation (Babiker and Baggott, 1995; Bakst  
389 and Holm, 2003). To our knowledge, the present study is the first to demonstrate the expression  
390 of carbonic anhydrase isoforms in the yolk sac. Calcium binding protein (CALB1) was reported  
391 to be essentially upregulated during the later stages of incubation, which we have corroborated,  
392 as seen in Figure 3 (Sechman et al., 1994; Yadgary et al., 2014). In addition, we observed a  
393 decrease in expression of GC between ED12 and ED16. These findings suggest that vitamin D  
394 uptake and calcium transport are mechanistically uncoupled. The vitamin D status of embryonic  
395 blood remains low up to hatching but may be concentrated in the bones (Nys et al., 1986).  
396 Indeed, vitamin D and a calcium-binding protein were shown to co-localize in dividing  
397 chondrocytes around hatch (Zhou et al., 1986). The uptake of vitamin D from the yolk during  
398 the first half of incubation and of eggshell calcium during the second half of incubation may  
399 correspond to highly orchestrated mechanisms that ultimately assist bone mineralization. In the  
400 yolk sac, we failed to detect TRPV6, a calcium selective channel that mediates Ca<sup>2+</sup> uptake in  
401 various tissues, including intestine and uterus of laying hens (Yang et al., 2011; Yang et al.,  
402 2013). TRPV6 was reported to decrease from ED11 to ED13 followed by an increase up to

403 ED19 in the yolk sac (Yadgary et al., 2011; Wong and Uni, 2021), but remarkably, its  
404 expression remains low between 10 and 15 days of incubation, and variability in later stages is  
405 surprisingly high (Yadgary et al., 2011). In view of these results, the physiological role of this  
406 calcium channel in calcium uptake from the eggshell and the yolk requires further study.

407

408 To conclude, the role of the yolk sac and the chorioallantoic membrane in transferring and  
409 transporting ions from yolk (phosphorus) and eggshell (calcium, magnesium and sodium),  
410 respectively, are complementary and involve distinct molecular components. These processes  
411 are associated with specialized cell types and their expression is temporally regulated in a  
412 coordinated manner. Both previous work and the novel results presented here highlight the need  
413 to consider the entire period of embryonic development, in order to have a more comprehensive  
414 picture of the relative functional roles of the CAM and the YS. None of the candidate genes  
415 encoding calcium binding proteins were shown to be significantly regulated during incubation:  
416 SCGN expression remains stable between the two developmental stages, CALB1 is not  
417 expressed in the CAM and TRPV6 expression is barely detectable. Thus, to date, the CAM  
418 proteins involved in the binding and transport of calcium from the eggshell to the embryo are  
419 not known. This example demonstrates the limitations of a candidate-gene approach. We are  
420 currently conducting a more systematic approach (RNA-Seq transcriptomics), which, combined  
421 with the localization of highly expressed genes within the CAM, will help to decipher the exact  
422 role of this multifunctional structure. We believe that the physiological and functional  
423 characterization of the CAM needs to be revisited using modern high-throughput techniques,  
424 similar to the strategy that has been used to explore the physiology of the yolk sac (Yadgary et  
425 al., 2014).

426 In addition to its interest in understanding the physiology of the extraembryonic structures  
427 which support embryonic development, this field of research may also have positive outputs

428 for the poultry industry. There is increasing evidence that intensive genetic selection of broiler  
429 breeders for meat production and layer hens for egg quality has precipitated the development  
430 of metabolic disorders including skeletal abnormalities (Thorp, 1994; Buzala et al., 2015;  
431 Eusemann et al., 2020). It is well known that skeletal integrity in chickens is affected by many  
432 factors including rapid growth rate, nutrition and genetics (Thorp, 1994). Fast growing broiler  
433 chicks exhibit impaired bone mechanical properties compared with slow-growing broiler chicks  
434 (Williams et al., 2000; Shim et al., 2012; Yair et al., 2017), while there is a very high prevalence  
435 of keel bone fractures in layer hens, regardless of the production system (Eusemann et al., 2020;  
436 Thøfner et al., 2021). Such bone pathologies compromise bird welfare and result in substantial  
437 economic losses for the poultry industry. The genetic determinants of bone and mineral  
438 metabolism are complex and involve multiple genetic loci (Mignon-Grasteau et al., 2016). The  
439 characterization of CAM and YS functions in skeletal mineralization of the embryo might help  
440 to identify *in ovo* markers as predictors of adult chicken bone health in modern poultry lines  
441 and lead to new selection tools.

442

443

## ACKNOWLEDGEMENTS

444 The authors are grateful to Sabine Alves (INRAE, IFC, PRC, Centre Val de Loire) for providing  
445 Rhodes Island eggs, to Joel Delaveau and Christophe Rat (INRAE, PEAT, Centre Val de Loire,  
446 DOI : 10.15454/1.5572326250887292E12) for egg handling and incubation and Anaïs Vitorino  
447 Carvalho for assistance with statistical analysis. The authors also thank “LE STUDIUM  
448 Institute for advanced studies - Loire Valley” for supporting the residency of M. Hincke at  
449 DOVE, BOA, INRAE Centre Val de Loire, and the Region Centre Val de Loire and the PHASE  
450 Department (INRAE) for the financing of M. Halgrain’s PhD. Hincke’s participation was  
451 additionally supported by the Canadian Natural Sciences and Engineering Research Council  
452 (NSERC, Discovery program RGPIN-2016-04410).

453

454

## CONFLICTS OF INTEREST

455 The authors declare no conflicts of interest.

456

457

## REFERENCES

458 Anderson, R.E., C.V. Gay, and H. Schraer. 1981. Ultrastructural localization of carbonic  
459 anhydrase in the chorioallantoic membrane by immunochemistry. *J. Histochem. Cytochem.*  
460 29(10):1121-1127.

461 Angel, R. 2007. Metabolic disorders: Limitations to growth of and mineral deposition into the  
462 broiler skeleton after hatch and potential implications for leg problems. *J. Appl. Poult. Res.*  
463 16(1):138–149.

464 Babiker, E. M., and G. K. Baggott. 1995. The role of ion transport in the formation of sub-  
465 embryonic fluid by the embryo of the Japanese quail. *Br. Poult. Sci.* 36(3):371-83.

466 Bakst, M. R., and L. Holm. 2003. Impact of egg storage on carbonic anhydrase activity during  
467 early embryogenesis in the turkey. *Poult. Sci.* 82(7):1193-1197.

468 Bauer, R., J. A. Plieschnig, T. Finkes, B. Riegler, M. Hermann, and W. J. Schneider. 2013. The  
469 developing chicken yolk sac acquires nutrient transport competence by an orchestrated  
470 differentiation process of its endodermal epithelial cells. *J. Biol. Chem.* 288(2):1088-1098.

471 Bellairs, R., and M. Osmond. 2014. *The atlas of chick development*. Ed, Academic Press,  
472 Oxford, UK.

473 Bond, G. M., R. G. Board, and V. D. Scott. 1988. A comparative study of changes in the fine  
474 structure of avian eggshells during incubation. *Zool. J. Linn. Soc.* 92(2):105-113.

475 Buzafa, M., B. Janicki, and R. Czarnecki. 2015. Consequences of different growth rates in  
476 broiler breeder and layer hens on embryogenesis, metabolism and metabolic rate: A review.  
477 *Poult. Sci.* 94(4):728-33.

478 Chien, Y. C., M. T. Hincke, H. Vali, and M. D. McKee. 2008. Ultrastructural matrix-mineral  
479 relationships in avian eggshell, and effects of osteopontin on calcite growth in vitro. *J. Struct.*  
480 *Biol.* 163(1):84-99.

481 Chien, Y. C., M. T. Hincke, and M. D. McKee. 2009. Ultrastructure of avian eggshell during  
482 resorption following egg fertilization. *J. Struct. Biol.* 168(3):527-538.

483 Clarkson, E. M., and M. Maizels. 1955. Sodium transfer in human and chicken erythrocytes. *J.*  
484 *Physiol.* 129(3):476-503.

485 Coleman, J. R., and A. R. Terepka. 1972a. Fine structural changes associated with the onset of  
486 calcium, sodium and water transport by the chick chorioallantoic membrane. *J. Membr. Biol.*  
487 7(1):111-127.

488 Coleman, J. R., and A. R. Terepka. 1972b. Electron probe analysis of the calcium distribution  
489 in cells of the embryonic chick chorioallantoic membrane. II. Demonstration of intracellular  
490 location during active transcellular transport. *J. Histochem. Cytochem.* 20(6):414-424.

491 Cusack, M., A. C. Fraser, and T. Stachel. 2003. Magnesium and phosphorus distribution in the  
492 avian eggshell. *Comp. Biochem. Physiol. B, Biochem. Mol. Biol.* 134(1):63-69.

493 Dennis, J. E., S. Q. Xiao, M. Agarwal, D. J. Fink, A. H. Heuer, and A. I. Caplan. 1996.  
494 Microstructure of matrix and mineral components of eggshells from White Leghorn chickens  
495 (*Gallus gallus*). *J. Morphol.* 228(3):287-306.

496 Dibner, J. J., J. D. Richards, M. L. Kitchell, and M. A. Quiroz. 2007. Metabolic challenges and  
497 early bone development. *J. Appl. Poult. Res.* 16(1):126-137.

498 Eusemann, B. K., A. Patt, L. Schrader, S. Weigend, C. Thöne-Reineke, and S. Petow. 2020.  
499 The role of egg production in the etiology of keel bone damage in Laying hens. *Front. Vet. Sci.*  
500 7:81.

501 Everaert, N., L. De Smit, M. Debonne, A. Witters, B. Kamers, E. Decuypere, and V.  
502 Bruggeman. 2008. Changes in acid-base balance and related physiological responses as a result  
503 of external hypercapnia during the second half of incubation in the chicken embryo. *Poult. Sci.*  
504 87(2):362-367.

505 Gabrielli, M. G. 2004. Carbonic Anhydrases in chick extra-embryonic structures: A role for CA  
506 in bicarbonate reabsorption through the chorioallantoic membrane. *J. Enzyme Inhib. Med.*  
507 *Chem.* 19(3):283-286.

508 Gabrielli, M. G., and D. Accili. 2010. The chick chorioallantoic membrane: A model of  
509 molecular, structural, and functional adaptation to transepithelial ion transport and barrier  
510 function during embryonic development. *J. Biomed. Biotechnol.* 2010.

511 Gabrielli, M. G., G. Materazzi, J. V. Cox, and G. Menghi. 2001. Specialised cell types in the  
512 chorioallantoic membrane express carbonic anhydrase during chick embryogenesis. *J. Anat.*  
513 198(2):229-238.

514 Gautron, J., M. T. Hincke, and Y. Nys. 1997. Precursor matrix proteins in the uterine fluid  
515 change with stages of eggshell formation in hens. *Connect. Tissue Res.* 36(3):195-210.

516 Gautron, J., L. Stapane, N. Le Roy, Y. Nys, A. B. Rodriguez-Navarro, and M. T. Hincke. 2021.  
517 Avian eggshell biomineralization: an update on its structure, mineralogy and protein tool kit.  
518 *BMC Mol. Cell Biol.* 22(1):11.

519 Gloux, A., N. Le Roy, A. Brionne, E. Bonin, A. Juanchich, G. Benzoni, M. L. Piketty, D. Prié,  
520 Y. Nys, J. Gautron, A. Narcy, and M. J. Duclos. 2019. Candidate genes of the transcellular and  
521 paracellular calcium absorption pathways in the small intestine of laying hens. *Poult. Sci.*  
522 98(11):6005-6018.

523 Hincke, M. T., M. Da Silva, N. Guyot, J. Gautron, M. D. McKee, R. Guabiraba-Brito, and S.  
524 Réhault-Godbert. 2019. Dynamics of structural barriers and innate immune components during  
525 incubation of the avian egg: Critical interplay between autonomous embryonic development  
526 and maternal anticipation. *J. Innate Immun.* 11(2):111-124.

527 Hincke, M. T., Y. Nys, J. Gautron, K. Mann, A. B. Rodriguez-Navarro, and M. D. McKee.  
528 2012. The eggshell: structure, composition and mineralization. *Front. Biosci.* 17(4):1266-80.

529 Hopcroft, R., A. J. Cowieson, W. I. Muir, and P. J. Groves. 2019. Changes to mineral levels in  
530 the yolk of meat chicken embryos during incubation. *Poult. Sci.* 98(3):1511-1516.

531 Jonchère, V., A. Brionne, J. Gautron, and Y. Nys. 2012. Identification of uterine ion transporters  
532 for mineralisation precursors of the avian eggshell. *BMC Physiol.* 12(1):10.

533 Karlsson, O., and C. Lilja. 2008. Eggshell structure, mode of development and growth rate in  
534 birds. *Zoology.* 111(6):494-502.

535 Kerschnitzki, M., A. Akiva, A. B. Shoham, N. Koifman, E. Shimoni, K. Rechav, A. A. Arraf,  
536 T. M. Schultheiss, Y. Talmon, E. Zelzer, S. Weiner, and L. Addadi. 2016. Transport of  
537 membrane-bound mineral particles in blood vessels during chicken embryonic bone  
538 development. *Bone.* 83:65-72.

539 Kidd, M. T. 2003. A treatise on chicken dam nutrition that impacts progeny. *World's Poult.*  
540 *Sci. J.* 59:475-494.

541 Kubota, M., E. Abe, T. Shinki and T. Suda. 1981. Vitamin D metabolism and its possible role  
542 in the developing chick embryo. *Biochem. J.* 194(1):103-109.

543 Kusumbe, A. P., S. K. Ramasamy, and R. H. Adams. 2014. Coupling of angiogenesis and  
544 osteogenesis by a specific vessel subtype in bone. *Nature.* 507(7492):323-328.

545 Lang, F., and E. Shumilina. 2013. Regulation of ion channels by the serum- and glucocorticoid-  
546 inducible kinase SGK1. *FASEB J.* 27(1):3-12.



547 Leeson, T. S., and C. R. Leeson. 1963. The chorio-allantois of the chick. Light and electron  
548 microscopic observations at various times of incubation. *J. Anat.* 97(4):585-595.

549 Maizels, M. 1954. Cation transport in chicken erythrocytes. *J. Physiol.* 125(2): 263-277.

550 Makanya, A. N., I. Dimova, T. Koller, B. Styp-Rekowska, and V. Djonov. 2016. Dynamics of  
551 the developing chick chorioallantoic membrane assessed by stereology, allometry,  
552 immunohistochemistry and molecular analysis. *PLoS ONE.* 11(4):e0152821.

553 Melkonian, G., N. Munoz, J. Chung, C. Tong, R. Marr, and P. Talbot. 2002. Capillary plexus  
554 development in the day five to day six chick chorioallantoic membrane is inhibited by  
555 cytochalasin D and suramin. *J. Exp. Zool.* 292(3):241-254.

556 Mignon-Grasteau, S., C. Chantry-Darmon, M. Y. Boscher, N. Sellier, M. Chabault-Dhuit, E.  
557 Le Bihan-Duval, and A. Narcy. 2016. Genetic determinism of bone and mineral metabolism in  
558 meat-type chickens: A QTL mapping study. *Bone Rep.* 5:43-50.

559 Narbaitz, R., B. Bastani, N. J. Galvin, V. K. Kapal, and D. Z. Levine. 1995. Ultrastructural and  
560 immunocytochemical evidence for the presence of polarised plasma membrane H<sup>+</sup>-ATPase in  
561 two specialised cell types in the chick embryo chorioallantoic membrane. *J. Anat.* 186:245-252.

562 Narbaitz, R., S. Kacew, and L. Sitwell. 1981. Carbonic anhydrase activity in the chick embryo  
563 chorioallantois: regional distribution and vitamin D regulation. *J. Embryol. Exp. Morphol.*  
564 65:127-137.

565 Narbaitz, R., and P. P. Tellier. 1974. The differentiation of the chick chorionic epithelium: an  
566 experimental study. *J. Embryol. Exp. Morphol.* 32(2):365-374.

567 Nys, Y., R. Bouillon, H. Van Baelen, and J. Williams. 1986. Ontogeny and oestradiol  
568 dependence of vitamin D-binding protein blood levels in chickens. *J. Endocrinol.* 108(1):81-  
569 87.

570 Nys, Y., M. T. Hincke, A. Hernandez-Hernandez, A. B. Rodriguez-Navarro, J. Gomez-  
571 Morales, V. Jonchère, J. M. Garcia-Ruiz, and J. Gautron. 2010. Structure, propriétés et

572 minéralisation de la coquille de l'œuf : rôle de la matrice organique dans le contrôle de sa  
573 fabrication. *INRA Prod. Anim.* 23(2):143-154.

574 Packard, M. J., N. B. Clark, and J. P. Erickson. 1998. The effect of calcium-regulating hormones  
575 on transport of calcium across the chorioallantoic membrane of the chicken embryo. *Comp.*  
576 *Biochem. Physiol. Part A Mol. Integr. Physiol.* 119(2):547-52.

577 Park, J. A., and S. H. Sohn. 2018. The influence of hen aging on eggshell ultrastructure and  
578 shell mineral components. *Korean J. Food Sci. Anim. Resour.* 38(5):1080-1091.

579 Peona, V., M. H. Weissensteiner, and A. Suh. 2018. How complete are "complete" genome  
580 assemblies? An avian perspective. *Mol. Ecol. Resour.* 18(6):1188-1195.

581 Richards, M. P. 1997. Trace mineral metabolism in the avian embryo. *Poult. Sci.* 76(1):152–  
582 164.

583 Rieder, E., C.V. Gay, and H. Schraer. 1980. Autoradiographic localization of carbonic  
584 anhydrase in the developing chorioallantoic membrane. *Anat. Embryol.* 159(1):17-31.

585 Rodríguez-Navarro, A. B., P. Marie, Y. Nys, M. T. Hincke, and J. Gautron. 2015. Amorphous  
586 calcium carbonate controls avian eggshell mineralization: A new paradigm for understanding  
587 rapid eggshell calcification. *J. Struct. Biol.* 190(3):291-303.

588 Romanoff, A. L. 1960. *The Avian Embryo. Structural and functional development.* The  
589 Macmillan Compagny, New York, USA.

590 Romanoff, A. L., and A. J. Romanoff. 1967. *Biochemistry of the avian embryo: a quantitative*  
591 *analysis of prenatal development.* Interscience Publishers.

592 Schaafsma, A., I. Pakan, G. J. H. Hofstede, F. A. J. Muskiet, E. Van Der Veer, and P. J. F. De  
593 Vries. 2000. Mineral, amino acid, and hormonal composition of chicken eggshell powder and  
594 the evaluation of its use in human nutrition. *Poult. Sci.* 79(12):1833-1838.

595 ScientificProtocols. 2014. Alizarin Red S (Bone) and Alcian Blue (Cartilage) staining of cleared  
596 skeletons. <http://doi.org/10.5281/zenodo.13517>.

597 Sechman, A., K. Shimada, N. Saito, T. Ieda, and T. Ono. 1994. Tissue-specific expression of  
598 calbindin-D28K gene during ontogeny of the chicken. *J. Exp. Zool.* 269(5):450-457.

599 Shen, T., and W. Chen. 2003. The role of magnesium and calcium in eggshell formation in  
600 Tsaiya ducks and Leghorn hens. *Anim. Biosci.* 16(2):290-296.

601 Shim, M. Y., A. B. Karnuah, A. D. Mitchell, N. B. Anthony, G. M. Pesti, and S. E. Aggrey.  
602 2012. The effects of growth rate on leg morphology and tibia breaking strength, mineral density,  
603 mineral content, and bone ash in broilers. *Poult. Sci.* 91(8):1790-1795.

604 Simons, P. C. M. 1971. Ultrastructure of the hen eggshell and its physiological interpretation.  
605 Centre for Agricultural Publishing and Documentation, Wageningen, the Netherlands.

606 Speake, B., A. Murray, and R. C. Noble. 1998. Transport and transformations of yolk lipids  
607 during development of the avian embryo. *Prog. Lipid Res.* 37(1):1-32.

608 Speier, J. S., L. Yadgary, Z. Uni, and E. A. Wong. 2012. Gene expression of nutrient  
609 transporters and digestive enzymes in the yolk sac membrane and small intestine of the  
610 developing embryonic chick. *Poult. Sci.* 91(8):1941-1949.

611 Stewart, M. E., and A. R. Terepka. 1969. Transport functions of the chick chorio-allantoic  
612 membrane. I. Normal histology and evidence for active electrolyte transport from the allantoic  
613 fluid, in vivo. *Exp. Cell Res.* 58(1):93-106.

614 Thøfner, I. C. N., J. Dahl, and J. P. Christensen. 2021. Keel bone fractures in Danish laying  
615 hens: Prevalence and risk factors. *PLoS One.* 16(8):e0256105.

616 Thorp, B. H. 1994. Skeletal disorders in the fowl: A review. *Avian Pathol.* 23(2):203-236.

617 Torres, C. A., and D. R. Korver. 2018. Influences of trace mineral nutrition and maternal flock  
618 age on broiler embryo bone development. *Poult. Sci.* 97(8):2996-3003.

619 Tuan, R. S. 1984. Carbonic anhydrase and calcium transport function of the chick embryonic  
620 chorioallantoic membrane. *Annals of the New York Academy of Sciences* 429(1):459-472.

621 Tuan, R. S., M. J. Carson, J. A. Josefiak, K. A. Knowles, and B. A. Shotwell. 1986. Calcium-  
622 transport function of the chick embryonic chorioallantoic membrane. I. *In vivo* and *in vitro*  
623 characterization. *J. Cell. Sci.* 82:73-84.

624 Tuan, R. S., and K. A. Knowles. 1984. Calcium-activated ATPase of the chick embryonic  
625 chorioallantoic membrane. Identification, developmental expression, and topographic  
626 relationship with calcium-binding protein. *J. Biol. Chem.* 259(5):2754-63.

627 Tuan, R. S., and T. Ono. 1986. Regulation of extraembryonic calcium mobilization by the  
628 developing chick embryo. *J. Embryol. Exp. Morphol.* 97:63-74.

629 Tuan, R. S. and J. Zrike. 1978. Functional Involvement of carbonic anhydrase in calcium  
630 transport of the chick chorioallantoic membrane. *Biochem. J.* 176(1):67-74.

631 Tyler C., and K. Simkiss. 1959. Studies on egg shells. XII. Some changes in the shell during  
632 incubation. *J. Sci. Food and Agric.* 10(11):611-615.

633 Uni, Z., L. Yadgary, and R. Yair. 2012. Nutritional limitations during poultry embryonic  
634 development. *J. Appl. Poult. Res.* 21(1):175-184.

635 Vandesompele, J., K. De Preter, F. Pattyn, B. Poppe, N. Van Roy, A. De Paepe, and F.  
636 Speleman. 2002. Accurate normalization of real-time quantitative RT-PCR data. *Genome Biol.*  
637 3(7):1-12.

638 Waddell, A. L., R. G. Board, V. D. Scott, and S. G. Tullett. 1989. Influence of dietary  
639 magnesium content on laying performance and egg shell magnesium content in domestic hen.  
640 *Br. Poult. Sci.* 30(4): 865-876.

641 Waddell, A. L., R. G. Board, V. D. Scott, and S. G. Tullett. 1991. Role of magnesium in  
642 egg shell formation in the domestic hen. *Br. Poult. Sci.* 32(4): 853-864.

643 Williams, B., S. Solomon, D. Waddington, B. Thorp, and C. Farquharson. 2000. Skeletal  
644 development in the meat-type chicken. *Br. Poult. Sci.* 41(2):141-9.

645 Wong, E. A., and Z. Uni. 2021. Centennial Review: The chicken yolk sac is a multifunctional  
646 organ. *Poult. Sci.* 100(3):100821.

647 Yadgary, L., R. Yair, and Z. Uni. 2011. The chick embryo yolk sac membrane expresses  
648 nutrient transporter and digestive enzyme genes. *Poult. Sci.* 90(2):410-416.

649 Yadgary, L., E. A. Wong, and Z. Uni. 2014. Temporal transcriptome analysis of the chicken  
650 embryo yolk sac. *BMC Genom.* 15(1):690-705.

651 Yair, R., A. Cahaner, Z. Uni, and R. Shahar. 2017. Maternal and genetic effects on broiler bone  
652 properties during incubation period. *Poult. Sci.* 96(7):2301-2311.

653 Yair, R., and Z. Uni. 2011. Content and uptake of minerals in the yolk of broiler embryos during  
654 incubation and effect of nutrient enrichment. *Poult. Sci.* 90(7):1523–1531.

655 Yair, R., Z. Uni, and R. Shahar. 2012. Bone characteristics of late-term embryonic and hatchling  
656 broilers: Bone development under extreme growth rate. *Poult. Sci.* 91(10):2614-2620.

657 Yang, J. H., J. F. Hou, C. Farquharson, Z. L. Zhou, Y. F. Deng, L. Wang, and Y. Yu. 2011.  
658 Localisation and expression of TRPV6 in all intestinal segments and kidney of laying hens. *Br.*  
659 *Poult. Sci.* 52(4):507-516.

660 Yang, J. H., Z. H. Zhao, J. F. Hou, Z. L. Zhou, Y. F. Deng, and J. J. Dai. 2013. Expression of  
661 TRPV6 and CaBP-D28k in the egg shell gland (uterus) during the oviposition cycle of the  
662 laying hen. *Br. Poult. Sci.* 54(3):398-406.

663 Zhou, X. Y., D. W. Dempster, S. L. Marion, J. W. Pike, M. R. Haussler, and T. L. Clemens.  
664 1986. Bone vitamin D-dependent calcium-binding protein is localized in chondrocytes of  
665 growth-plate cartilage. *Calcif. Tissue Int.* 38(4):244-247.

666 Table 1: Information related to candidate genes.

Symbol	Gene ID	Gene Name	Function	Subcellular location	Primer Sequence 5'- 3'	Amplicon size (bp)
CA2*	396257	Carbonic anhydrase 2	Bone resorption and osteoclast differentiation. Hydration of carbon dioxide and intracellular pH regulation	Cytosol/plasma membrane	Fw :ATCGTCAACAACGGGCACTCCTTC	101
					Rev :TGCACCAACCTGTAGACTCCATCC	
CA4	417647	Carbonic anhydrase 4	Hydration of carbon dioxide, stimulation of the sodium/bicarbonate transporter activity of SLC4A4 (pH homeostasis)	Plasma membrane	Fw :GGAAGCAAACAGTCACCCATC	225
					Rev :GACTCCCCAGTGCAGATGAAA	
CA9	770004	Carbonic anhydrase 9	Hydration of carbon dioxide, pH regulation	Plasma membrane	Fw :CCTGACAACCTGCACCTCTA	159
					Rev :GAGGTGGTTGTCGTCTGTCT	
PKD2	422585	Polycystin 2, transient receptor potential cation channel	Component of a heteromeric calcium-permeable ion channel formed by PKD1 and PKD2	Plasma membrane	Fw :ACCTGAGAAGTGTTTTGCGG	122
					Rev :GAGCTGCGACATAACCCTCG	
SLC4A1	396532	Solute carrier family 4 member 1	Mediation of chloride-bicarbonate exchange in the kidney, urine acidification	Plasma membrane	Fw :TGAGACCTTCGCCAAACTCG	291
					Rev :TTCAGCTTCTGCGTGTAGGT	
ATP6V1B2	395497	ATPase H <sup>+</sup> transporting V1 subunit B2	Acidification of intracellular compartments-organelles	Cytosol	Fw :CCCCACAATGAGATTGCAGC	171
					Rev :CATGGACCCATTTTCCTCAAAGTC	
SGK1	395133	Serum/glucocorticoid regulated kinase 1	Regulation of various ion channels, renal Na <sup>+</sup> /K <sup>+</sup> and intestinal Na <sup>+</sup> /H <sup>+</sup> exchange and nutrient transport	Nucleus	Fw :GCCAGTCCATCACAAACAGA	124
					Rev :ATGCCGTGCAAGAAGAACCT	
TRPV6	427502	Transient receptor potential cation channel, subfamily V, member 6	Mediation of Ca <sup>2+</sup> uptake in various tissues, Ca <sup>2+</sup> ion homeostasis (body and bones)	Plasma membrane	Fw :CACTCCTTCAAGCTGCCAAG	242
					Rev :CTGGTTCAGTCTGCAATGT	
CALB1*	396519	Calbindin-1	Intracellular Ca <sup>2+</sup> binding protein	Cytosol	Fw :CAGGGTGTCAAATGTGTGC	215
					Rev :GCCAGTTCTGCTCGGTAAAG	
GC	395696	GC vitamin D binding protein	Vitamin D transport and storage	Secreted	Fw :TAGCAACTCACGCCGAACAC	95
					Rev :CATGGCTCGGAAGTCATCCTT	
SCGN	421001	Secretagogen, EF-hand calcium binding protein	Regulation of calcium ion concentration	Cytosol	Fw :GATGGACGTCTGGACCTGAA	221
					Rev :CCACTGATGCTGGGCTTGAC	

667 \* Primer sequences from Jonchère et al., 2012. Fw, forward; Rev, reverse

668 Table 2: Eggshell physical characteristics and mineral content for two stages of embryo  
 669 development (ED12 vs ED16) (n=30 per stage). P-values lesser than 0.05 were considered as  
 670 significant (in bold type) with arrows to describe the evolution between both stages.

		ED12	ED16	p-value
Initial egg weight (g)		64.46 ± 1.85	63.95 ± 1.99	0.3669
Egg weight at sampling (g)		60.4 ± 1.81	58.82 ± 2.09	<b>0.0034</b> ↓
<b>Eggshell physical characteristics</b>	Strength (N)	39.79 ± 4.69	34.01 ± 4.92	<b>&lt;.0001</b> ↓
	Eggshell weight (g)	6.31 ± 0.47	6.01 ± 0.44	<b>0.0133</b> ↓
	Thickness (mm)	0.47 ± 0.03	0.43 ± 0.03	<b>&lt;.0001</b> ↓
<b>Eggshell mineral content (mg)*</b>	P	6.78 ± 0.93	6.49 ± 0.88	0.1872
	Mg	19.59 ± 3.39	17.86 ± 2.90	<b>0.0112</b> ↓
	K	2.65 ± 0.35	2.54 ± 0.29	0.1124
	Na	6.43 ± 0.70	6.03 ± 0.65	<b>0.0307</b> ↓
	Ca	2298.49 ± 191.01	2171.66 ± 182.39	<b>&lt;0.01</b> ↓

671 \* For the eggshell mineral content, values correspond to those of the total shell

672

673

674 **Figure legends**

675 **Figure 1:** Staining of embryo skeletons with Alcian blue and Alizarin red at ED12 (A) and  
676 ED16 (B) (representative results, n=30 per stage). Blue color reveals the cartilaginous parts; in  
677 red/purple, the mineralized bones. Arrows indicate regions undergoing an increase in  
678 mineralization between the two stages of development. 1, cervical vertebra; 2, ribs; 3, ilium; 4,  
679 caudal vertebra; 5, ischium; 6, digits of the legs.

680

681 **Figure 2.** RT-qPCR (n=18 per stage) of candidate genes in the CAM. A. Carbonic anhydrases  
682 (CA2, CA4, CA9), ion transporters and regulators (SLC4A1, ATP6V1B2, SGK1, SCGN,  
683 PKD2). B. TRPV6 (gene that is not expressed in the yolk sac). Experiments were conducted  
684 according to Materials and Methods. Normalized quantity was determined using five  
685 housekeeping genes as described in Materials and Methods.

686

687 **Figure 3.** RT-qPCR (n=18 per stage) of candidate genes in the YS. A. Carbonic anhydrases  
688 (CA2, CA4, CA9), ion transporters and regulators (SLC4A1, ATP6V1B2, SGK1, SCGN,  
689 PKD2). B. CALB1 and vitamin-D binding protein (GC). Experiments were conducted  
690 according to Materials and Methods. Normalized quantity was determined using only one  
691 housekeeping gene (ACTB) as described above due to the extreme variability of the other  
692 housekeeping gene candidates in the yolk sac at ED12 and ED16.

693

694 **Figure 4.** Hypothetical representation of the role of candidate genes in the chorionic epithelium  
695 of the CAM (A) and in the YS (B) during the second half of incubation, in mineral mobilization  
696 from the eggshell and the yolk, respectively. This model integrates the literature (detailed in the



697 discussion section) and the expression data obtained in the present study. A. The CAM is  
698 composed of three distinct layers (A) where the chorionic epithelium is assumed to be involved  
699 in the transepithelial ion transport (Gabielli and Accili, 2010) from the blood (red rectangle)  
700 and the eggshell (grey rectangle). In this scheme inspired by Gabielli and Accili, 2010, VC  
701 cells are specialized chorionic cells, which, via a vacuolar-type H<sup>+</sup>-ATPase present at the apical  
702 pole (ATP6V1V2), pump protons generated by cytoplasmic carbonic anhydrases (CA2, CA4  
703 and CA9) towards the eggshell (step ①). Proton secretion results in a local acidification (step  
704 ②), thereby causing solubilization of the calcite mineral (step ③). HCO<sup>3-</sup> is proposed to be  
705 reabsorbed through VC cells via the anion exchanger SLC4A1, to maintain acid-base-balance  
706 within the CAM. Ca<sup>2+</sup> and other ions including HCO<sup>3-</sup>, Mg<sup>2+</sup> and Na<sup>+</sup> become available to be  
707 reabsorbed via by CC cells, for transport via the vasculature to the embryo. Our results suggest  
708 that ions transporters such as SCGN and PKD2 participate in Ca<sup>2+</sup> binding and transport;  
709 however, CALB1 expression was not detected at ED12 or ED16. The very low expression of  
710 TRPV6 in the CAM brings into question the role of this candidate gene in calcium uptake.  
711 SGK1 may be involved in Na<sup>+</sup> transport while the transporter for Mg<sup>2+</sup> is not yet known. As  
712 expected, since the eggshell does not contain vitamin D, the GC gene is not expressed in the  
713 CAM. B. In the yolk sac, carbonic anhydrases (CA2, CA4, CA9) and a proton-pumping ATPase  
714 (ATP6V1V2) contribute to the acid-base balance of YS cells and the yolk (step ①). Minerals  
715 and vitamin D are absorbed from the yolk (yellow rectangle) to the blood (red arrows), via the  
716 transporters expressed by the YS (CALB1, SCGN, PKD2, SGK1, GC - step ②). TRPV6 in  
717 not expressed in YS at ED12 or ED16 (~~TRPV6~~). In these proposed mechanisms (A and B),  
718 erythrocytes may also express CA2, SLC4A1 and SGK1.

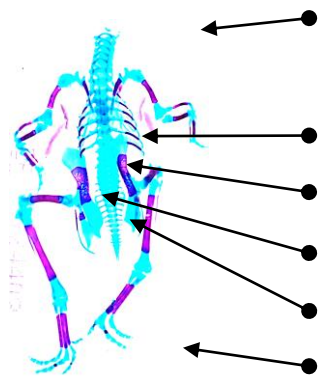
719 Schematic representation of the CAM and the YS (left part) is inspired by Hincke et al. (2019)  
720 and Bauer et al. (2013). Some elements were obtained from Servier Medical Art  
721 (<https://smart.servier.com>), licensed under a Creative Commons Attribution 3.0 Unported

722 License. CC, capillary covering cells; VC, villous cavity cells. Grey arrows illustrate the  
723 transport from the blood to the eggshell via the CAM or the yolk via the yolk sac, and red arrows  
724 illustrate transport into the blood vessels.

725 It must be emphasized that the intact yolk sac and CAM tissues were analyzed: endoderm,  
726 mesoderm, and ectoderm for the yolk sac, and allantoic epithelium, mesoderm and chorionic  
727 epithelium for the CAM. Each candidate gene in this study may be differentially expressed in  
728 the various layers or cell types (Discussion section). Hence, the specific localization of all  
729 candidate genes and proteins in YS and CAM will require further experimental study.

730

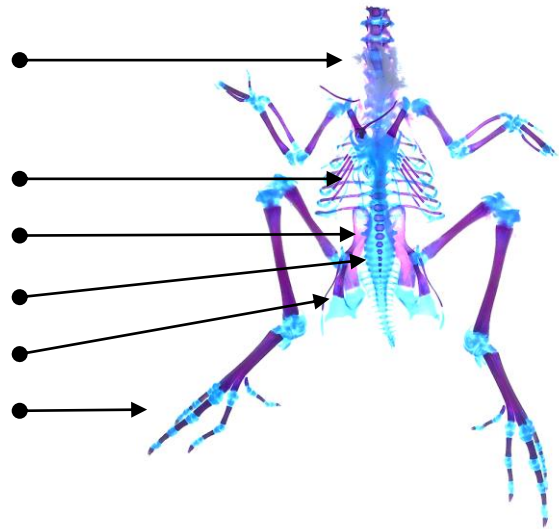
**A**



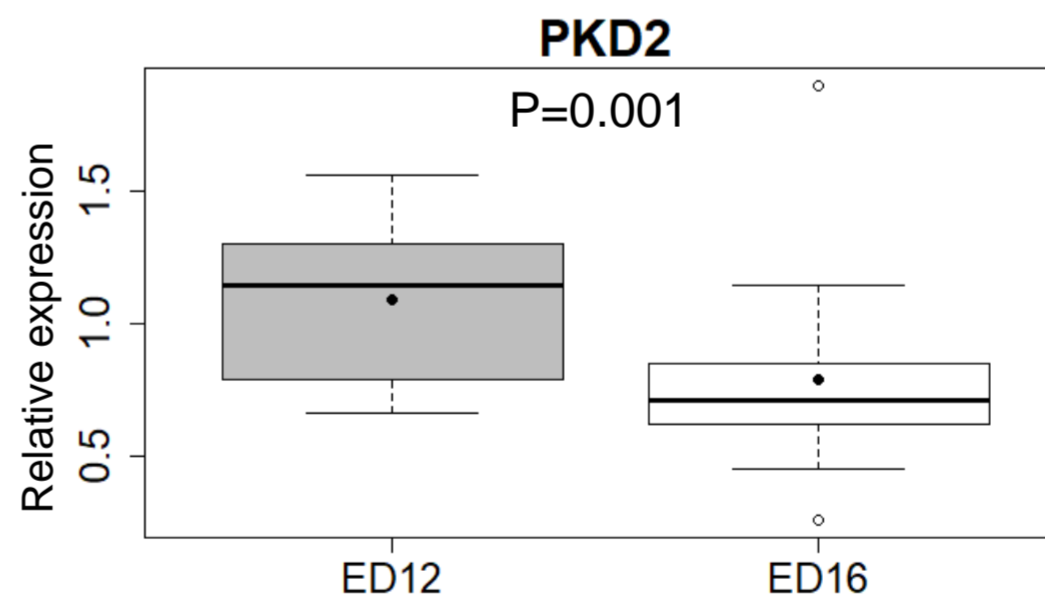
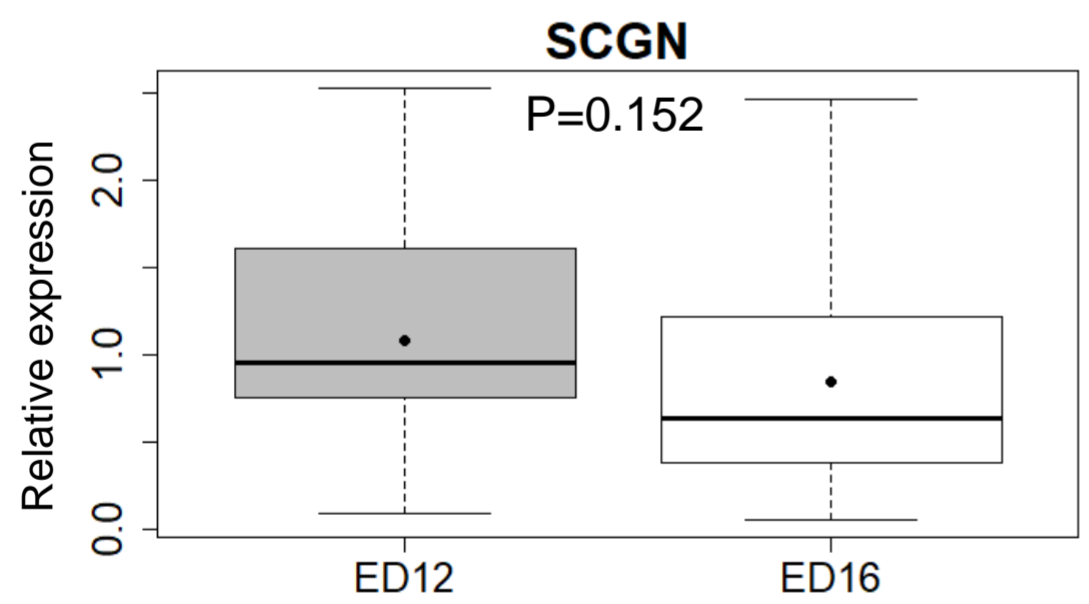
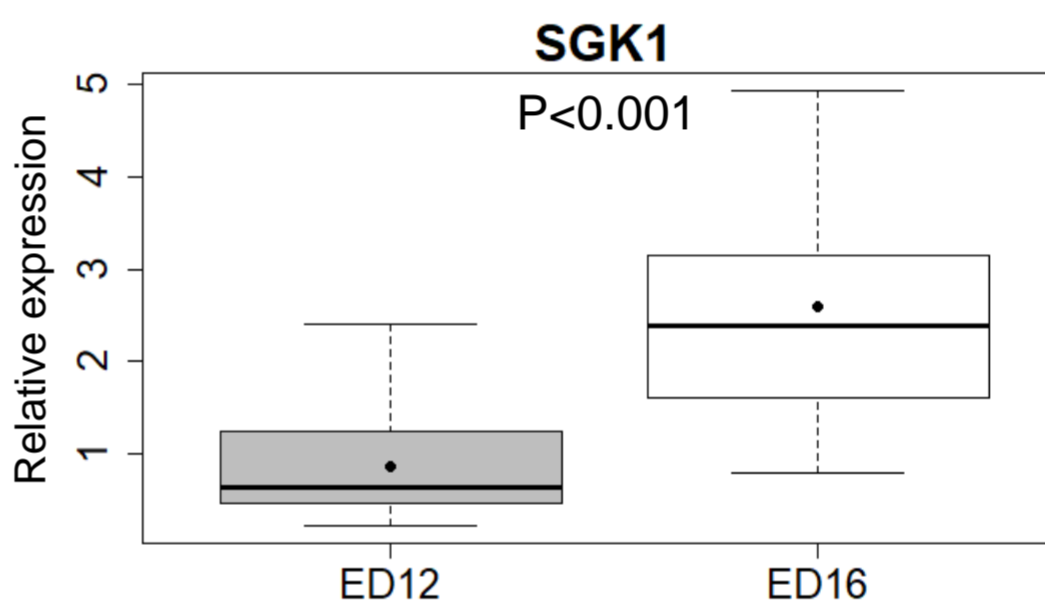
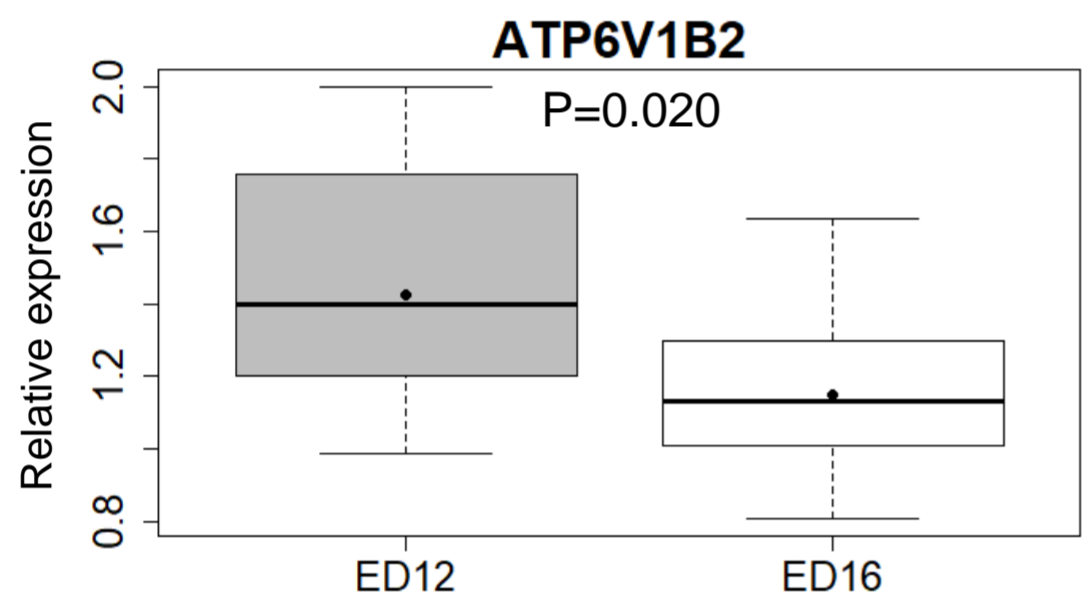
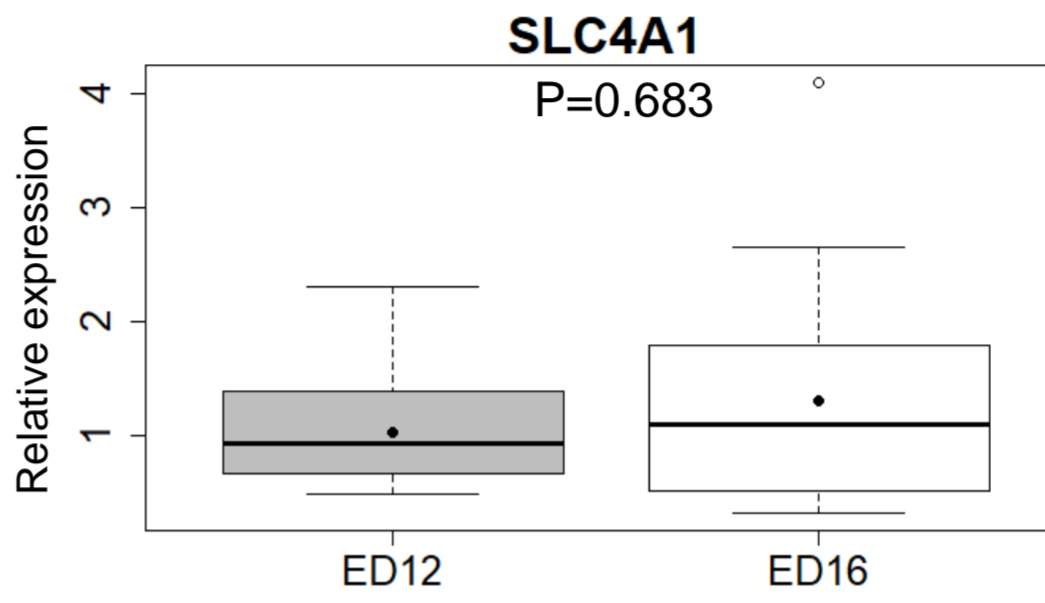
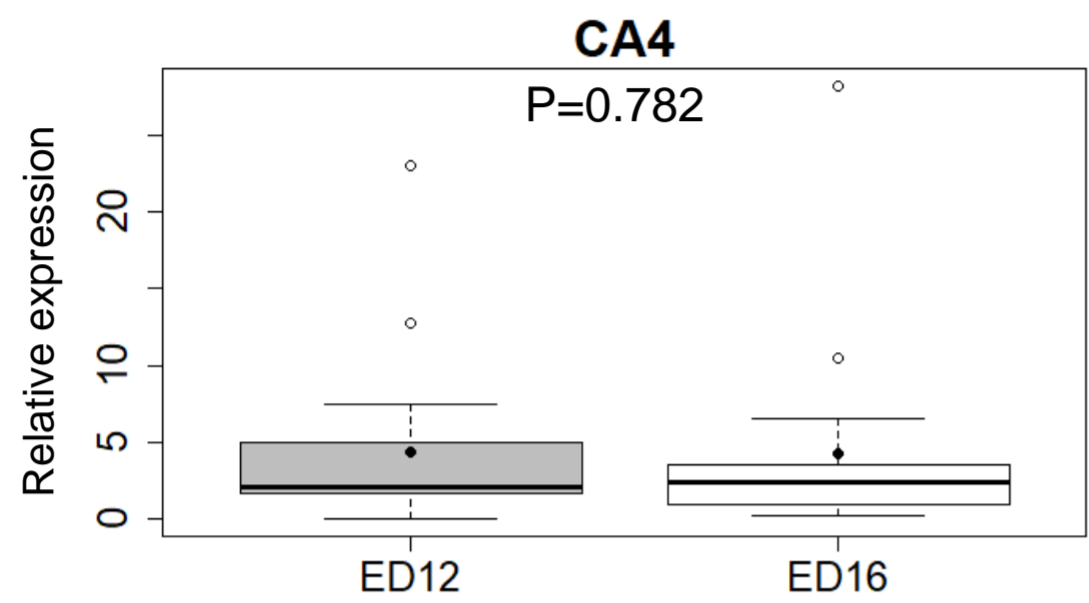
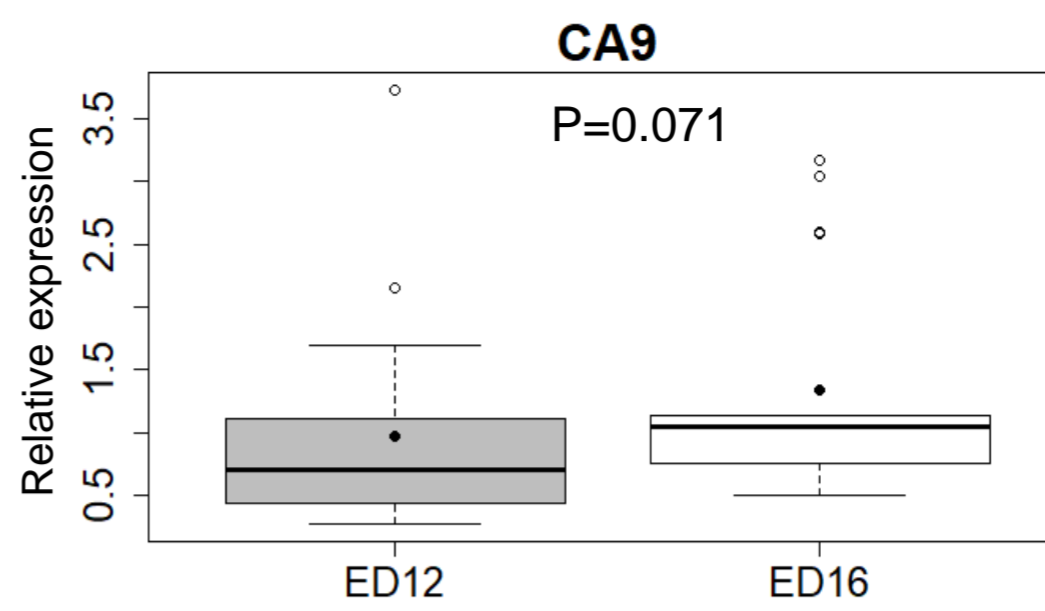
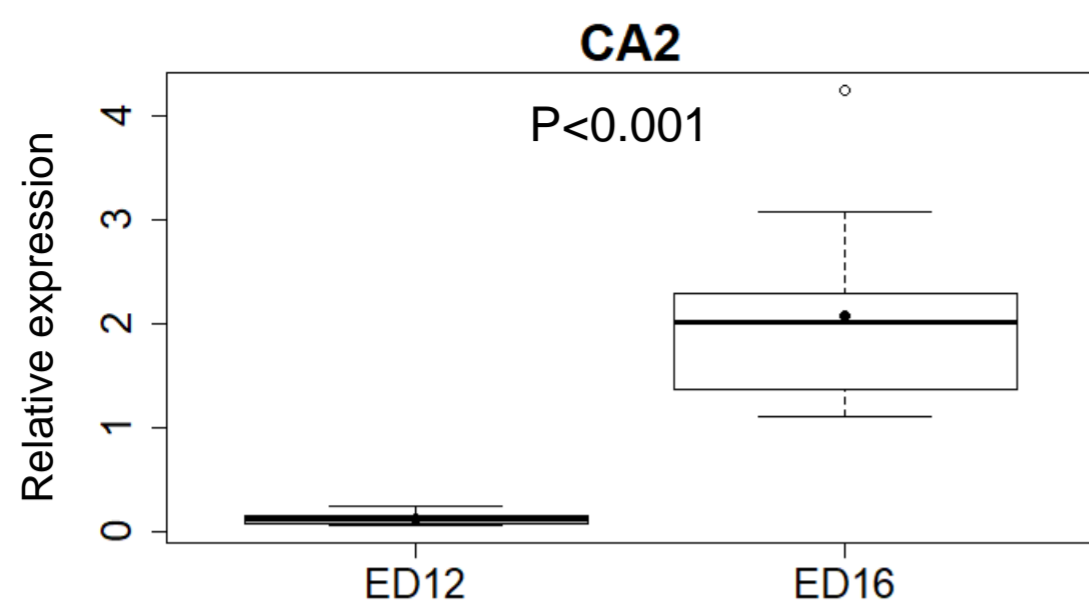
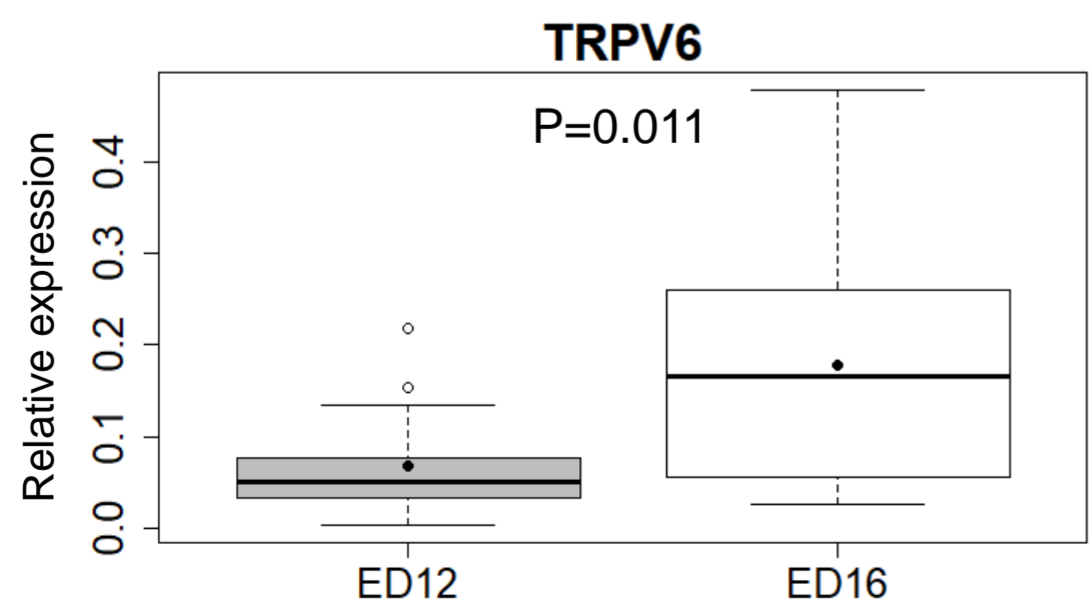
1 cm



**B**



**Figure 1**

**A****B**

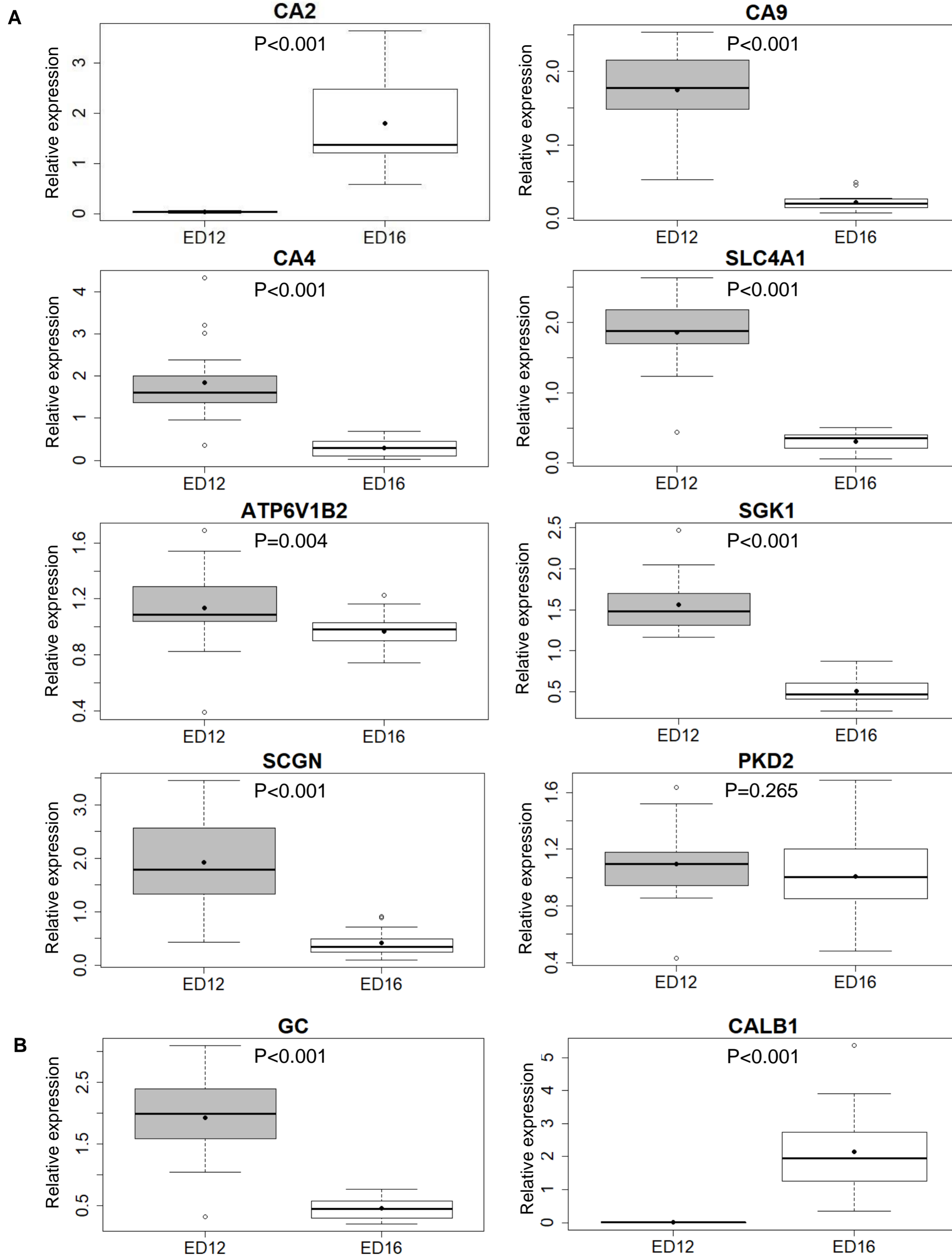
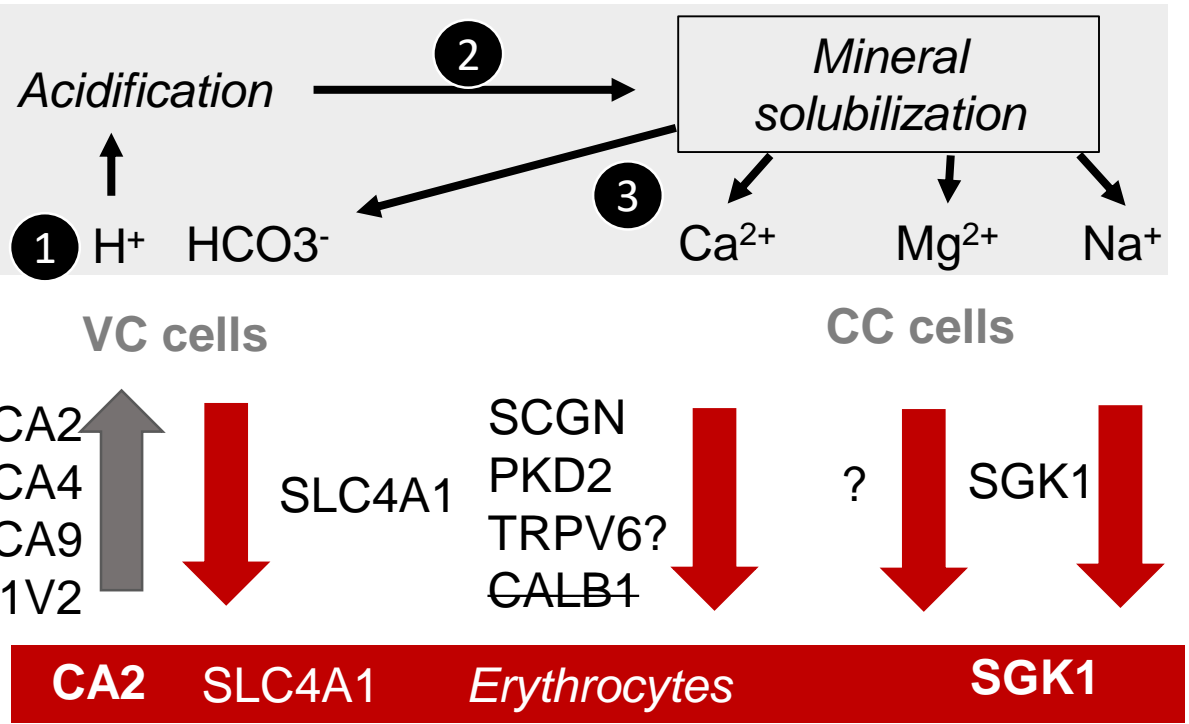
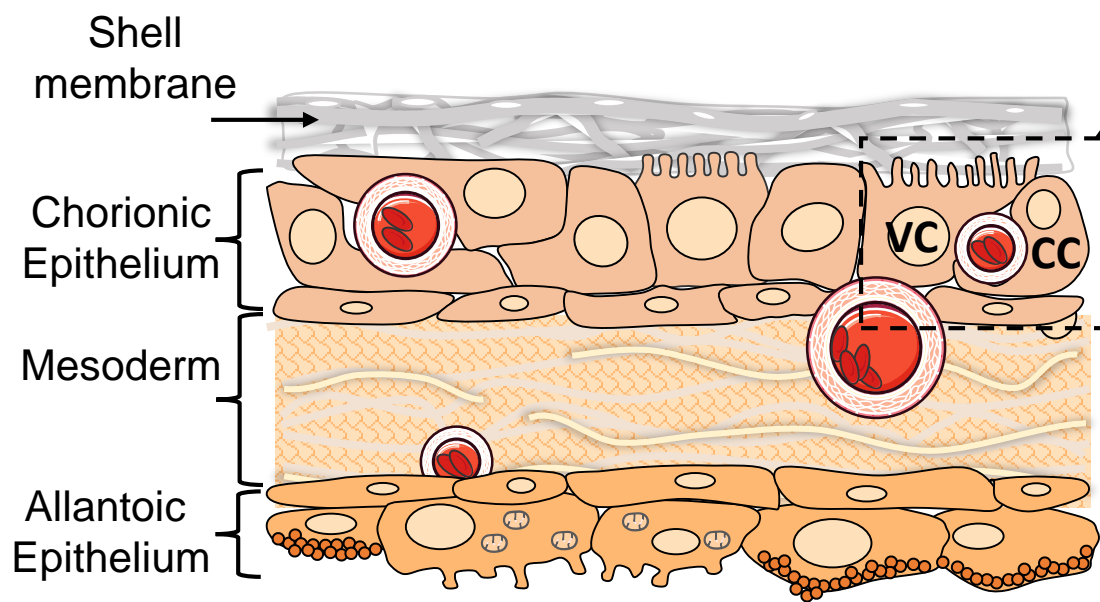


Figure 3

### A Chorioallantoic membrane at ED16



### B Yolk sac at ED16

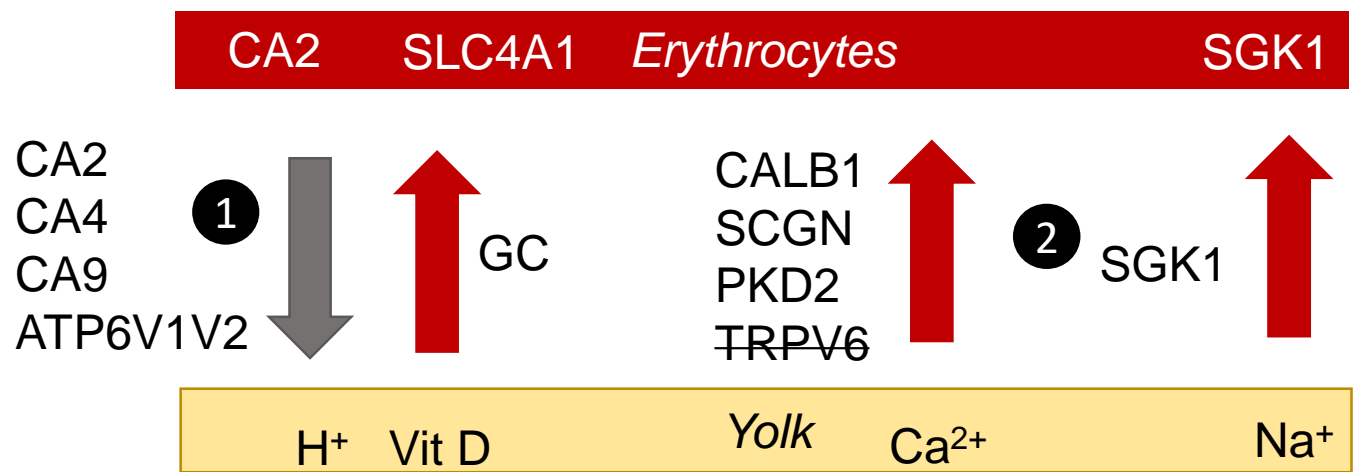
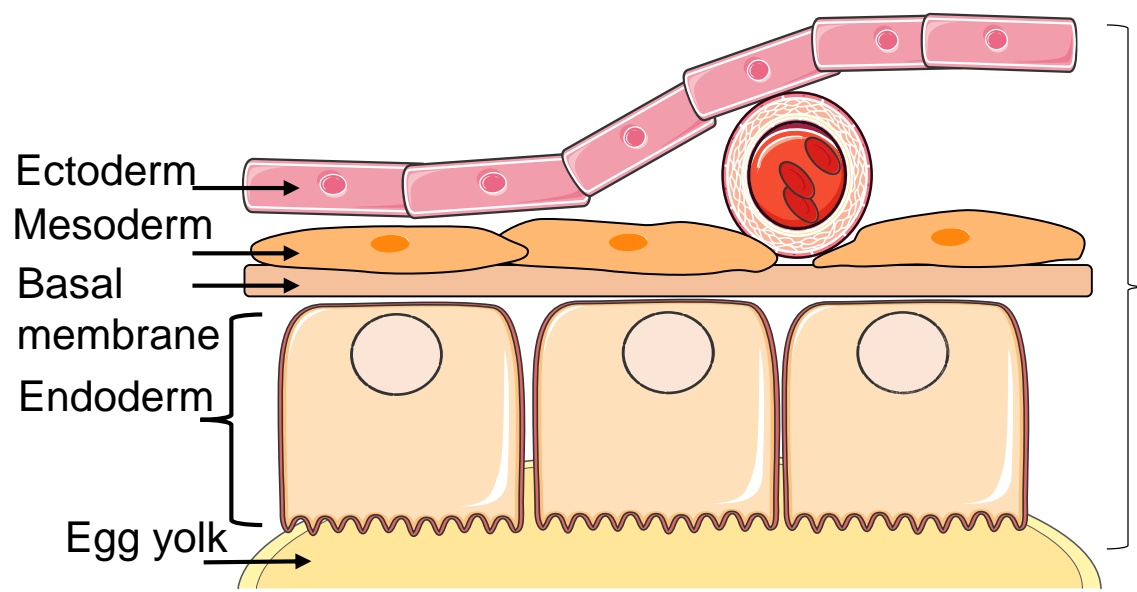


Figure 4